



Antarctic winter sea-ice seasonal simulation with a coupled model: Evaluation of mean features and biases

P P SAHEED^{1,2,*}, ASHIS K MITRA¹, IMRANALI M MOMIN¹ and VIMLESH PANT²

¹*National Centre for Medium Range Weather Forecasting, Ministry of Earth Sciences, Noida, UP, India.*

²*Centre for Atmospheric Sciences, Indian Institute of Technology Delhi, New Delhi, India.*

*Corresponding author. e-mail: saheed@ncmrwf.gov.in

MS received 4 January 2021; revised 15 June 2021; accepted 16 June 2021

For Earth's climate system, the study of the seasonal variability of sea-ice is important as the sea-ice has a significant impact on the net radiative flux, which can influence the mean seasonal behaviours of the atmosphere and ocean. In this study, the seasonal hindcast of 14 austral winter seasons is conducted to assess the skill of a coupled model in simulating the seasonal Antarctic sea-ice and its connection with the other ocean and atmospheric variables. The GloSea4 set-up of the HadGEM3 coupled model is used for the seasonal simulations at the NCMRWF. The model could reproduce the sea-ice extent over the Antarctic for the Austral winter seasons with an average correlation value of 0.98. However, there are moderate biases in the sea-ice concentration. The sea-ice thickness in the model generally shows negative bias, which is not seen to be related to the surface air temperature biases in the coupled system. The moderate positive (warm) biases in the sea surface temperature extending into the upper ocean (30 m), combined with the sea-ice drift bias pattern away from the sea-ice region are the main reasons for the underestimation of sea-ice thickness in the model. The sea surface current bias pattern shows a poleward component that brings the warm water from the warm biased locations of the exterior region into the sea-ice region and explains the presence of warmer waters in the sea-ice regions. The anti-clockwise bias in the surface wind is seen to impact the surface current, Antarctic circumpolar current (ACC), having a similar anti-clockwise current bias. Despite these moderate biases in the model, the inter-annual variability of sea-ice extent is having a reasonably good skill. The model is suitable for extended/seasonal prediction of sea-ice during Austral winter for Antarctic.

Keywords. Antarctic sea-ice; model simulation; coupled model; sea-ice verification.

1. Introduction

Sea-ice forms between the ocean and atmospheric interface, formidably blocking the interaction between these two fluids. Sea-ice variability in different time scales is one of the most direct climate change indicators (Feltham 2015). The high surface albedo associated with the sea-ice restricts a considerable amount of solar radiation reaching

the ocean beneath the sea-ice; hence it plays a significant role in regulating the global heat budget. The Antarctic continent and the surrounding Antarctic Ocean, and the Southern Ocean, have a significant role in the Earth's climate system. The accurate prediction of weather/climate patterns in the Antarctic is vital for conducting field studies and logistical operations in the Antarctic, and it is a challenging scientific and technical problem.

There are fewer studies on Antarctic climate change than the Arctic, although significant climate changes have happened in the Antarctic in the last few decades. The Antarctic sea-ice extent shows a distinct annual cycle reaching maximum in September in the Austral winter and minimum in February in the Austral summer (figure 1). The seasonal variability of Antarctic sea-ice extent varies from a maximum value of 19 million km² in September to a minimum value of 3 million km² in February (Cavalieri and Parkinson 2008). The Antarctic sea-ice shows a growing trend from 1979 through 2010, as the satellite multichannel passive-microwave record revealed (Parkinson and Cavalieri 2012). After 2010, record-high sea-ice extent months in the Antarctic were reported by Parkinson Claire and DiGirolamo (2016). They found high sea-ice extent in four months (August–November) of 2013, six months (April–September) of 2014, and three months (January, April, and May) of 2015. The increasing trend in sea-ice had a setback in 2016 with a dramatic turn reporting a record-low sea-ice extent in the Antarctic. The rate at which the Antarctic sea-ice has been decreasing since then is faster than the sea-ice retreat that happened in the Arctic (Parkinson 2019). Coupled ocean-atmosphere-sea-ice simulation models are useful tools to study the variability of sea-ice and related climate variables. However, the skill of the climate simulation models needs to be evaluated. The present study aims to assess the sea-ice and related ocean and atmospheric seasonal simulation using the coupled model, HadGEM3 (Hewitt *et al.* 2011) in its seasonal setup (GloSea4) (Arribas *et al.* 2011). The model simulations were compared with the satellite and reanalysis datasets. The seasonal hindcasts for 14 seasons are conducted during the period 1996–2009. In this study, the model

hindcast evaluation is done for July, August, and September (JAS). The mean JAS months represent the peak freezing period where maximum variability in the Antarctic sea-ice distribution is seen.

2. Coupled model set-up and data used

In a seamless modelling approach, the same dynamical code and the same parameterization schemes (wherever possible) are used across a broad range of spatial and temporal scales on a traceable framework. The same model is used for numerical weather prediction (NWP), extended range prediction and seasonal forecasting, and climate modelling with forecast time scales ranging from a few days to hundreds of years, and it can also be applied to both global and regional scales. At the National Centre for Medium Range Weather Forecasting (NCMRWF), a coupled model is set up with a similar configuration as the GloSea4 system of UKMO (Arribas *et al.* 2011). The basic model framework is the HadGEM3 (Hadley Centre Global Environment Model version 3) model of UKMO. The HadGEM3 model (Hewitt *et al.* 2011) framework comprises an atmospheric model, Unified Model (UM), Nucleus of European Modelling of the Ocean (NEMO) ocean model, and the Los Alamos National Laboratory community-driven sea-ice model (CICE). These three models are coupled using the OASIS coupler. The atmospheric model has a spatial resolution of 1.875°×1.25° in the horizontal, with 85 layers in the vertical (50 levels are below 18 km). The NEMO ocean model has a spatial resolution of 1°×1° in horizontal and 75 vertical layers with a very fine resolution in the ocean near-surface. The NEMO model (Madec 2008) employs ORCA tripolar grid configuration. The bathymetry for the NEMO model is derived from the ETOPO2 data set (2'' global bathymetry). The sea-ice model, CICE (Hunke and Lipscomb 2008), is based on the zero-layer approximation of Semtner (1976). The CICE model has five ice thickness categories (ITD) in each grid cells. The model computes the ice growth and melt rates in multi-layer (Bitz and Lipscomb 1999). However, this version of the HadGEM3 set-up uses the zero-layer thermodynamic model of Semtner (1976) with one layer of snow and one layer of ice in the vertical. Global Ice 6.0 configuration of the CICE model is explained by Rae *et al.* (2015). In this study, the global coupled seasonal hindcast runs are performed from

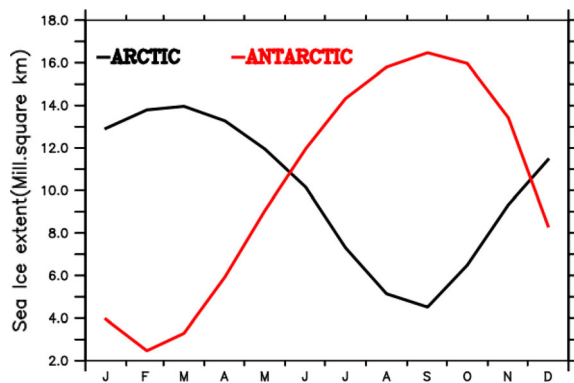


Figure 1. Climatology of sea-ice extent, Arctic (black line) and Antarctic (red line).

1996 to 2009 with 9th May initial condition and extending to October each year. The heat, freshwater, and momentum fluxes are exchanged between the different components (UM, NEMO, and CICE models) of HadGEM3 through the OASIS coupler every 3 hours. Solar, longwave and turbulent (sensible and latent) fluxes are exchanged between the atmosphere and the ocean. Sea-ice, at its top surface, is melted due to the exchange of heat with the atmosphere and at its bottom surface, the growth or melt is due to the exchange of heat with the ocean. Freshwater is exchanged in the form of rain and snow from the atmosphere model or from the sea-ice model where ice is present. Freshwater flux is created between the ocean and the sea-ice when the sea-ice is formed or melted. More technical details of the HadGEM3 model is explained by Hewitt *et al.* (2011).

The results of July, August, and September (JAS), the months of Austral winter, are discussed in this study. The focus of this study is to assess the skills of the model in simulating the sea-ice in the Antarctic ocean. A similar study for the Arctic region was reported earlier by Saheed *et al.* (2018).

The HadISST1 (Rayner *et al.* 2003) sea-ice concentration data of Met Office Hadley Centre is used as the observed data to compare with the model simulated sea-ice concentration and sea-ice extent. The GIOMAS dataset (Zhang and Rothrock 2003), containing sea-ice motion vectors and sea-ice thickness information, is also used to compare with the model simulation. The ERA INTERIM dataset (Dee *et al.* 2011) is used for the atmospheric variables, 10 m winds, and 2 m temperature. The ECMWF Ocean Reanalysis (ORAP5) dataset (Balmaseda *et al.* 2013) is used for ocean vertical temperature comparison with the model, and the Reynolds's SST (Reynolds *et al.* 2007) datasets are used for sea surface temperature (SST) comparison with the model.

3. Results and discussion

The sea-ice and related oceanic and atmospheric variables from the coupled model are discussed over the Antarctic Ocean for the Austral winter season of July, August, and September (JAS) from 1996 through 2009. The peak winter for the southern polar region is associated with the JAS months, during which the sea-ice extent is usually approaching its maximum (figure 1) as these are months of intense freezing over Antarctica and the

surrounding ocean. The cold air temperature causes the sea-ice formation, and it expands in a far stretch reaching beyond the 60°S (equatorward). This expansion of sea-ice is critical to be simulated by the model. The model's biases will indicate the skill of the model to reproduce the sea-ice and the governing mechanism of sea-ice formation.

3.1 Sea-ice and ocean surface features

The sea-ice concentration, represented in fraction, is a crucial parameter to examine in the model simulations. Figure 2 shows the mean sea-ice concentration in the observed (a), model (b), and the model bias (c). The spatial coverage of sea-ice concentration in both the model and the observation is showing a similar pattern. A positive bias distribution up to 0.5 is seen in the sea-ice edges in the Atlantic–Indian Ocean sector. A positive bias of 0.2 is seen in the Pacific sector of the Antarctic. There are a few negative bias patches with values up to -0.2 in the Amundsen Sea and the Ross Sea, the western Antarctic, and the King Haakon VII Sea. These negative bias values in the interior western Antarctic Circle are consistent with the sea-ice thickness bias (figure 3).

Figure 3 shows the mean sea-ice thickness in the observed (a), model (b), and the model bias (c). Both in the observation and the model, the maximum sea-ice thickness values are seen in the western Antarctic. In the observation, a maximum of 2-m thick ice is seen near the Ronne Ice Shelf, whereas, in the model, the maximum thickness values are seen near the Larsen Ice Shelf. In the observation, 1.75–2 m thick ice is seen in the Amundsen Sea and the Ross Sea, but the model underestimates the sea-ice thickness in these regions. The sea-ice thickness is gradually reduced from the Antarctic Peninsula towards the Southern Ocean both in the observation and the model. The model predicted sea-ice thickness in the entire Antarctic Ocean is less compared to observation. The negative bias values, ranging from -0.5 to -1.0 m, are seen in the entire Antarctic. The only exception is the region near the Larsen Ice Shelf, where the model shows a positive bias. The maximum sea-ice thickness values (positive bias) in the model near the Larsen Ice Shelf can be attributed to the sea-ice drift bias pattern (figure 5c). The sea-ice drift is against the Larsen Ice Shelf, which could produce thick ice due to the sea-ice ridging process. Similarly, there is a drift pattern away from the

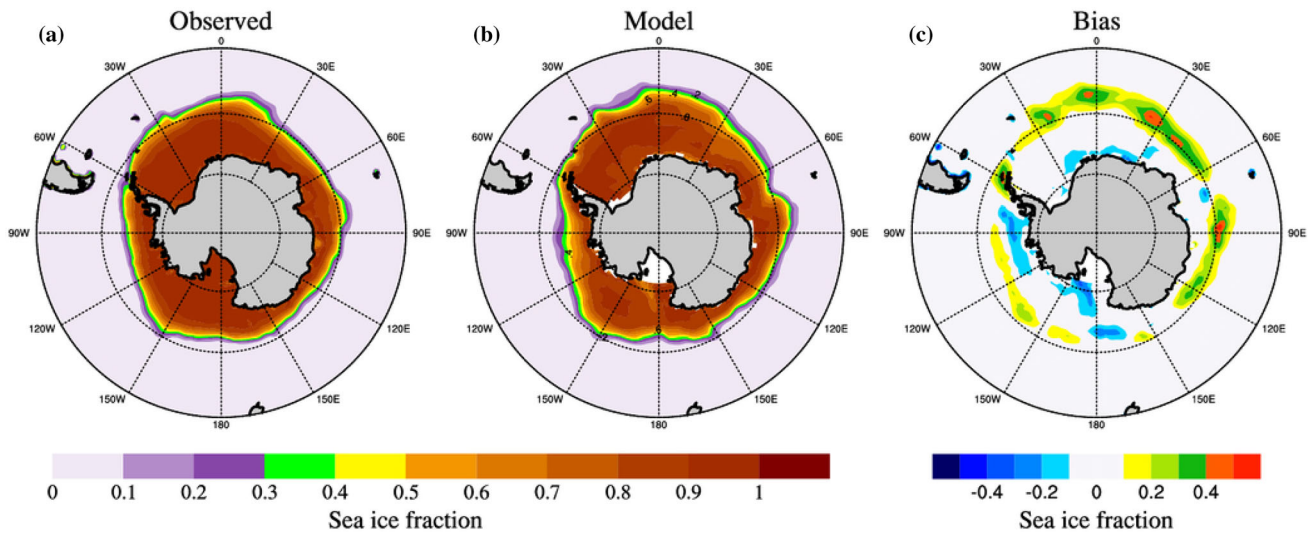


Figure 2. Mean sea-ice concentration (JAS) during 1996–2009: (a) observed, (b) model, and (c) bias.

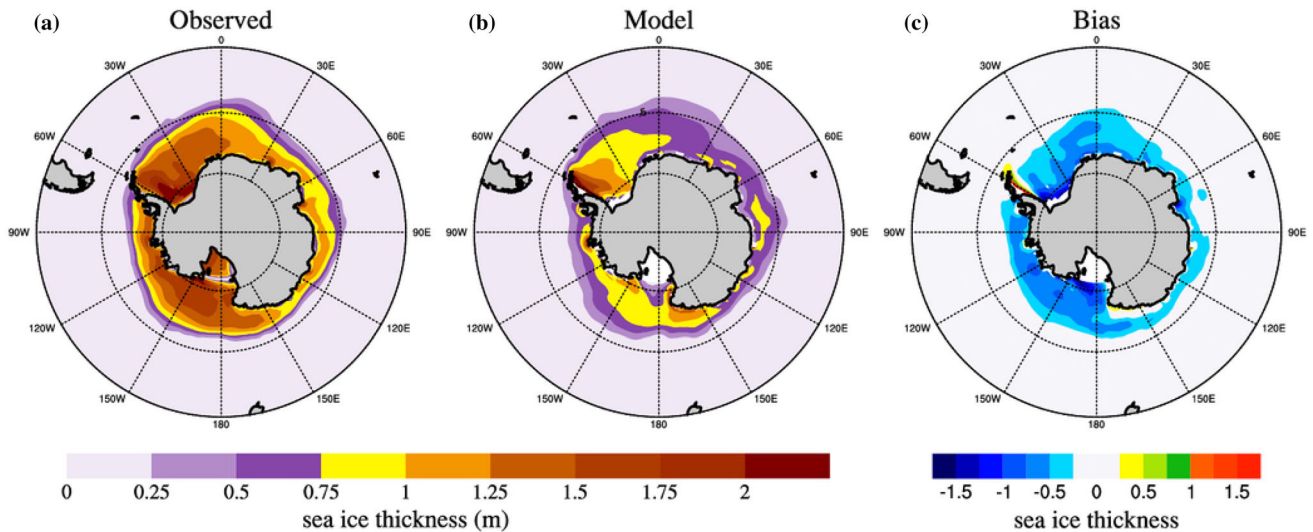


Figure 3. Mean sea-ice thickness (JAS) during 1996–2009: (a) observed, (b) model, and (c) bias.

Ronne Ice Shelf, which results in the underestimation of sea-ice thickness in this region. In the Amundsen Sea and the Ross Sea regions, there is a strong sea-ice drift bias pattern away from the sea-ice region, which could be the reason for the underestimation of sea-ice thickness by the model. In figure 4, the sea surface current bias shows a poleward component that can bring warm water from the southern ocean (lower latitude). That could be one of the possible reasons for the reduced sea-ice thickness (negative bias). The bias in the sea-ice drift pattern (figure 5c) shows a drift away from the Antarctic ice region, and this can also be a reason for the negative bias in the sea-ice thickness distribution. The air temperature (figure 6) shows

a similar negative (cooler) bias as the sea-ice thickness (figure 3), indicating that the bias in sea-ice thickness is not related to the air temperature bias and hence could be related to the ocean-sea-ice processes.

Figure 4 shows the seasonal (JAS) mean surface currents in the observed (a), model (b), and model bias (c). In the observation, the Antarctic ocean circulation is featured with the Antarctic circumpolar current (ACC), the largest ocean circulation, which is also known as west-wind drift. The ACC flows clockwise from the west to east direction around Antarctica, making it the largest ocean current. The maximum intensity of the ACC is seen around the Antarctic peninsula and

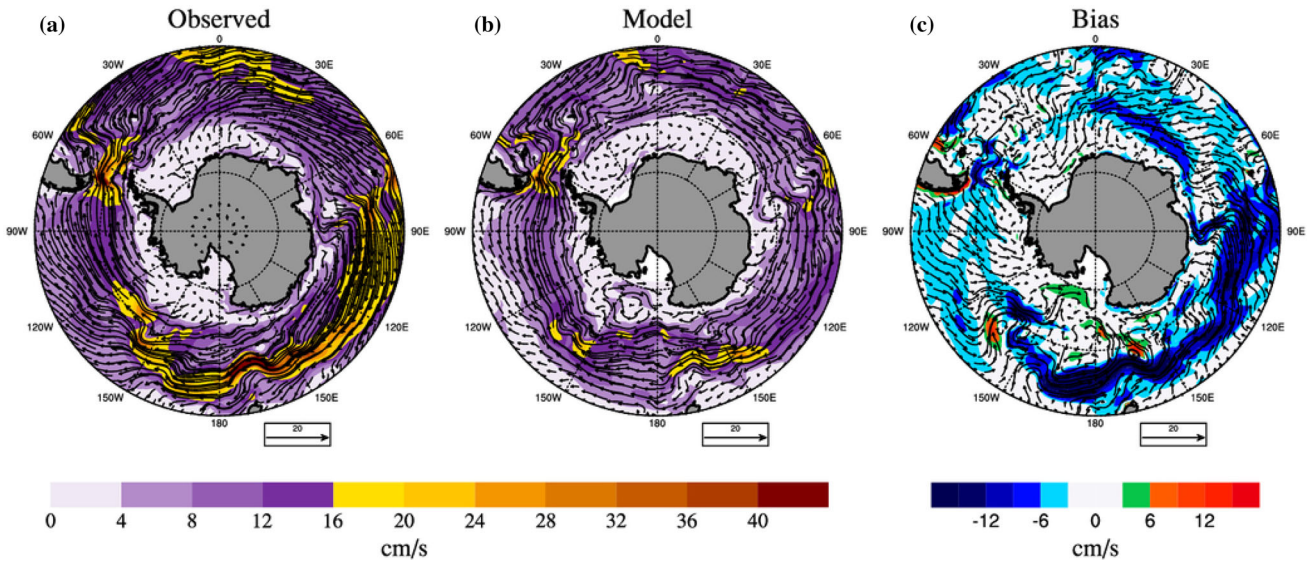


Figure 4. Mean surface current (JAS) during 1996–2009: (a) observed, (b) model, and (c) bias.

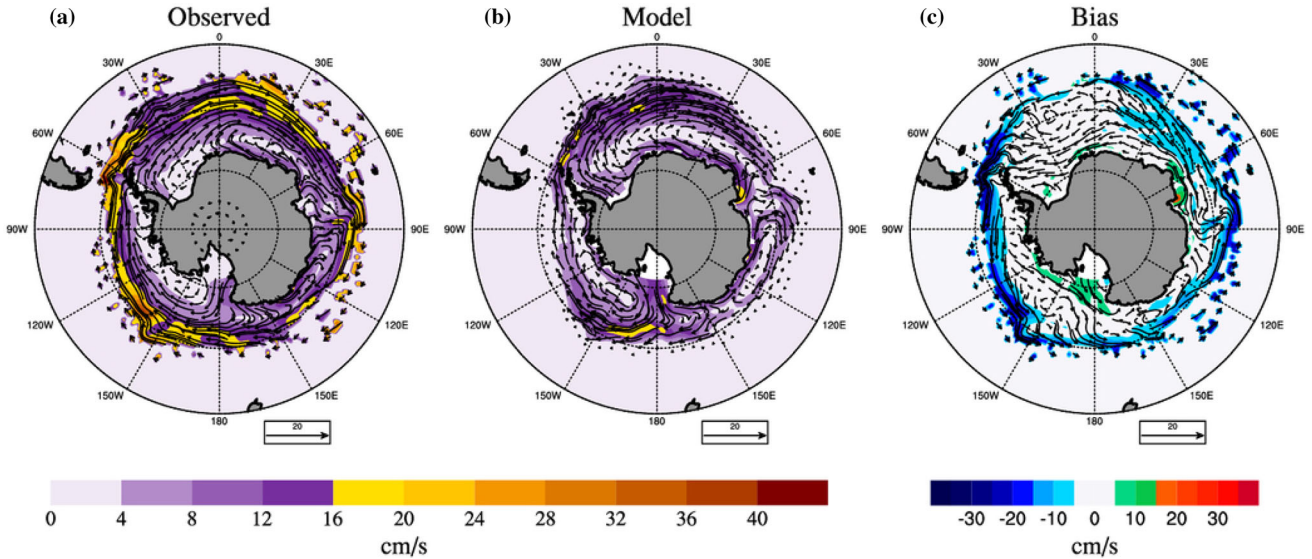


Figure 5. Mean sea-ice drift (JAS) during 1996–2009: (a) observed, (b) model, and (c) bias.

in the Antarctic circle’s outer boundaries. The model simulations produce the ACC pattern well. However, the intensity of the circulation is slightly underestimated all over the region around Antarctica. There is a clockwise eddy near the Ross Sea in the model simulation, which is missing in the observation. There is an anti-clockwise circulation pattern with a poleward component all over the Antarctic region in the bias. This poleward component can bring warm water from the exterior sea-ice regions and influence the sea-ice distribution, as discussed earlier. This negative bias in ACC is due to the negative bias in the 10-m winds (figure 7).

Figure 5 shows the seasonal (JAS) mean sea-ice drift in the observed (a), model (b), and model bias (c). Strong drift velocities characterize the observed sea-ice drift out of the Ross Sea and the Weddell Sea. In the Antarctic circle outline, the sea-ice drift is following the ACC. The sea-ice drift out of the Ross Sea is overestimated in the model seasonal simulation. Similar to the surface current bias (figure 4), there is an anti-clockwise pattern (counter direction of ACC) in the sea-ice drift. However, there is also a drift component away from the sea-ice region, which could be one reason for the negative bias in the sea-ice thickness (figure 3). Drifting of sea-ice against the shelf region causes

sea-ice ridging, and thick ice is formed. When the drift is away from the sea-ice region, sea-ice thins. Here, as discussed earlier, the contrasting biases near the Larsen Ice Shelf and the Ronne Ice Shelf regions in the western Antarctic, and the negative biases in the Amundsen Sea and Ross Sea regions, can be attributed to the sea-ice drift biases in the model.

3.2 Atmospheric features

Figure 6 shows the seasonal (JAS) mean air-temperature in the observed (a), model (b), and model bias (c). Very low air-temperature values

characterize the Austral winter season in the southern polar region. In the observation, a low air temperature value of -30°C is seen, which is well simulated by the model despite few negative bias patches with values up to -4°C in the Ross Sea and the Weddell Sea. A widespread negative bias of -1°C is seen in the interior regions of the Antarctic circle, especially in the Amundsen Sea and the western Pacific Ocean sector. There is a small positive bias patch of 3°C in the Ross Sea region. The cold bias in surface temperature is due to the negative bias in the surface wind, which cannot transport the cold air efficiently away from the poles. The air temperature bias shows the same

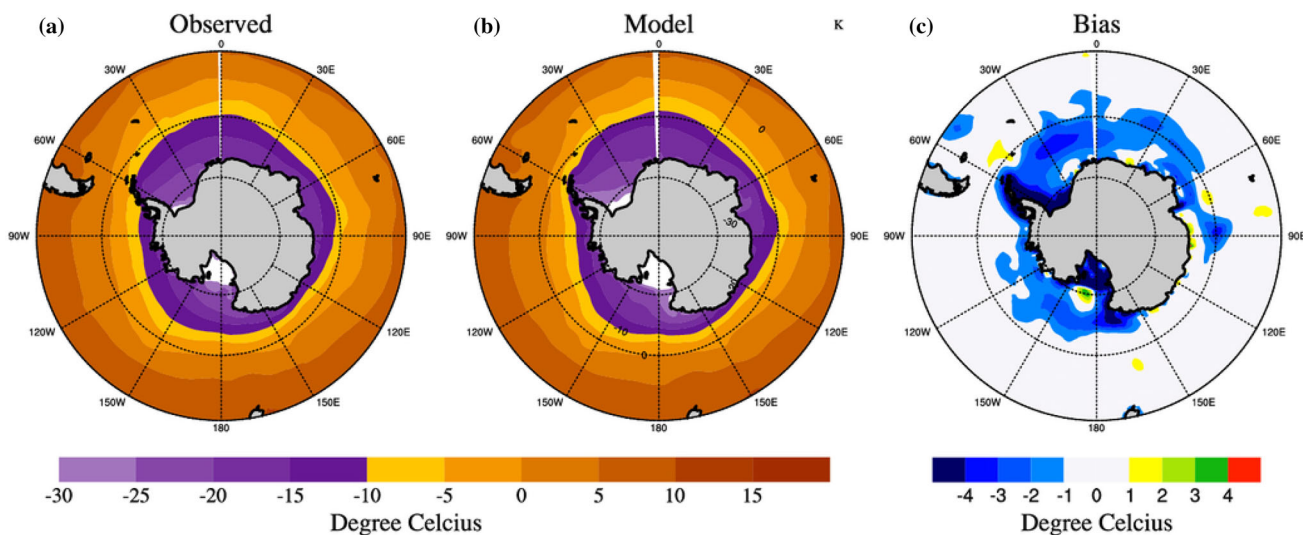


Figure 6. Mean air temperature at 2 m (JAS) during 1996–2009: (a) observed, (b) model, and (c) bias.

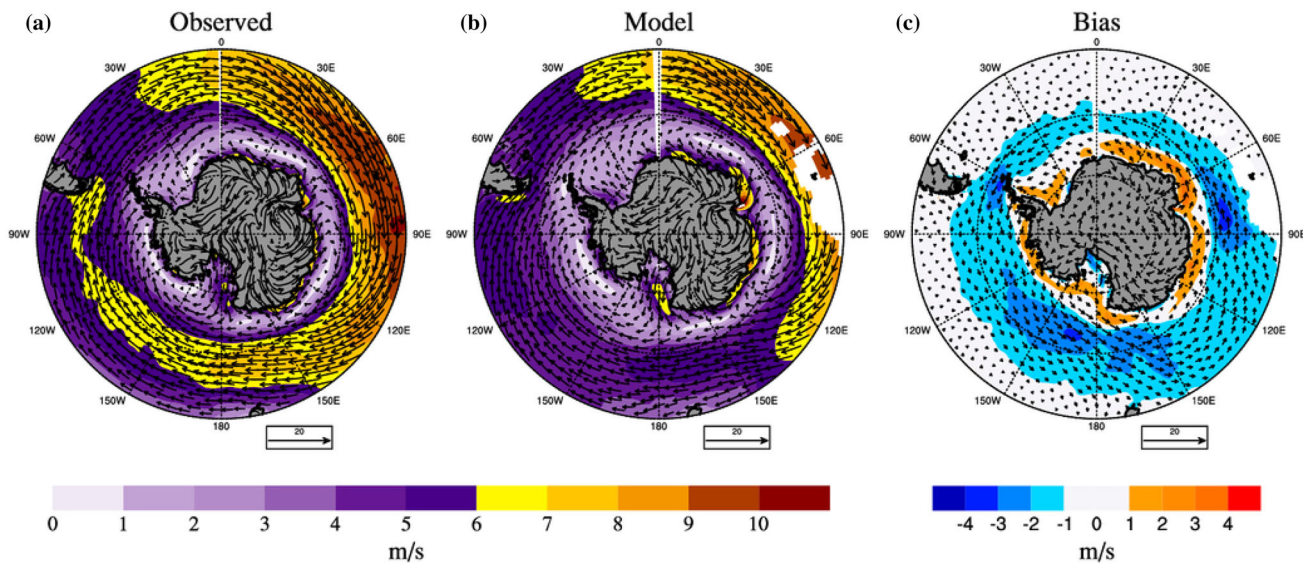


Figure 7. Mean 10 m wind (JAS) during 1996–2009: (a) observed, (b) model, and (c) bias.

sign as that of the sea-ice thickness. So, the negative bias in the air temperature is not the reason for the sea-ice thickness bias.

Figure 7 shows the seasonal (JAS) mean 10-m wind in the observed (a), model (b), and model bias (c). The Antarctic Ocean near-surface atmospheric circulation flows in a clockwise direction, driving the ACC in the west to east. The model seasonal forecast also shows a similar atmospheric circulation pattern. However, the intensity of the clockwise circulation is less compared to that of the observation. There is a feeble counter-clockwise circulation pattern around Antarctica in the bias. This counter-clockwise pattern is consistent with the sea surface current (i.e., ACC) and sea-ice drift biases.

3.3 Ocean surface and sub-surface features

Figure 8 shows the seasonal (JAS) mean of sea surface temperature (SST) in the observed (a), model (b), and the model bias overlaid with the model sea surface current bias (c). In the observation, a low SST value of -2°C is seen in most of the Antarctic circle, over the sea-ice regions. The SST is getting warmer away from the sea-ice region, towards the Southern Ocean. The model is also showing a similar pattern in the seasonal simulation. There are patches of positive bias in the Weddell Sea, the Ross Sea, the Amundsen Sea, and the eastern Antarctic region in the Indian Ocean Sector. There are negative bias patches in the northern Weddell Sea and many places in the

outer sea-ice region. There is a slight positive (warm) bias in the model in most sea-ice regions (figure 2). The overlaid sea-surface current bias over the SST bias (figure 8c) shows poleward sea surface current vectors from the warm bias outer sea-ice regions, which causes the intrusion of warm water into the sea-ice region. This warm water intrusion can limit sea-ice growth, resulting in the underestimation of sea-ice thickness in the model.

Figures 9 and 10 show the seasonal (JAS) mean of sub-surface ocean temperature at 12 and 30 m depths, respectively, in the observed (a), model (b), and model bias (c). The sub-surface temperature at 12 and 30 m depths in the observation shows a similar pattern as the surface temperature getting warmer when moving away from the sea-ice region. The subsurface temperature bias patterns in the 12 and 30 m depths show a similar pattern as seen in SST. However, the warm bias in the sub-surface is a bit stronger in the sea-ice region compared to the SST. The subsurface temperature bias figures also substantiate the fact that there is a spread of warm water from the warmer bias regions into the sea-ice area, affecting sea-ice growth in the model. The temperature distribution at 30-m depth does not differ from the temperature at 12 m depth in the Antarctic Ocean as both the levels show almost the same pattern indicating both levels may be within the upper layer having similar characteristics. From figures 9 and 10 (sub-surface temperature biases), we can conclude that the sub-surface ocean also affects the underestimation of sea-ice thickness in the model.

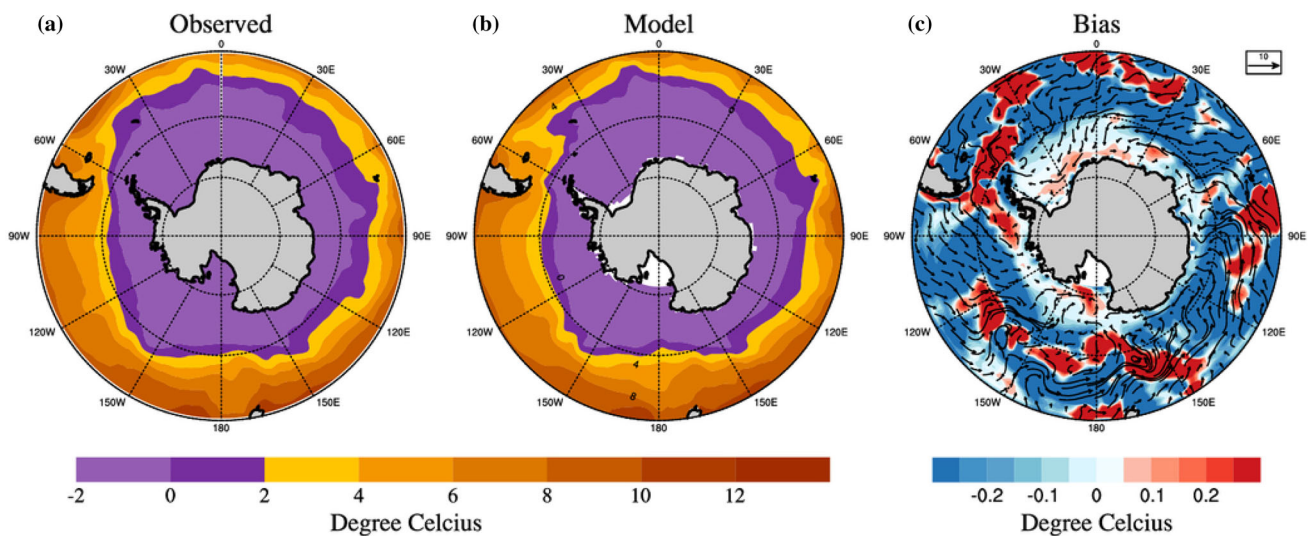


Figure 8. Mean SST (JAS) during 1996–2009: (a) observed, (b) model, and (c) SST bias, overlaid with surface current bias.

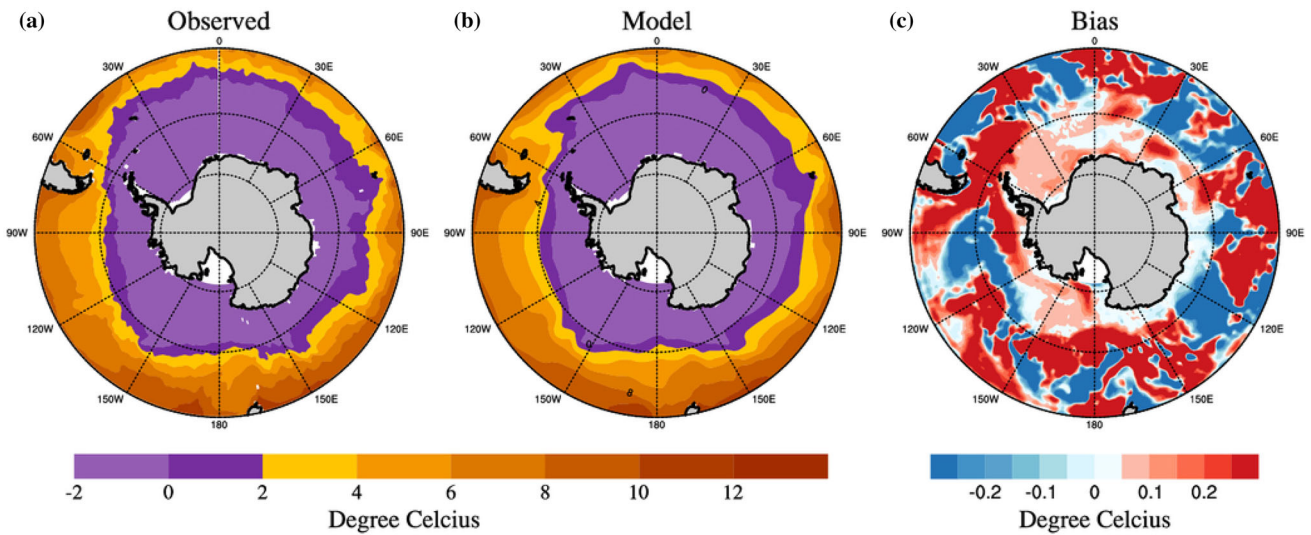


Figure 9. Mean sub-surface temperature at 12 m (JAS) during 1996–2009: (a) observed, (b) model, and (c) bias.

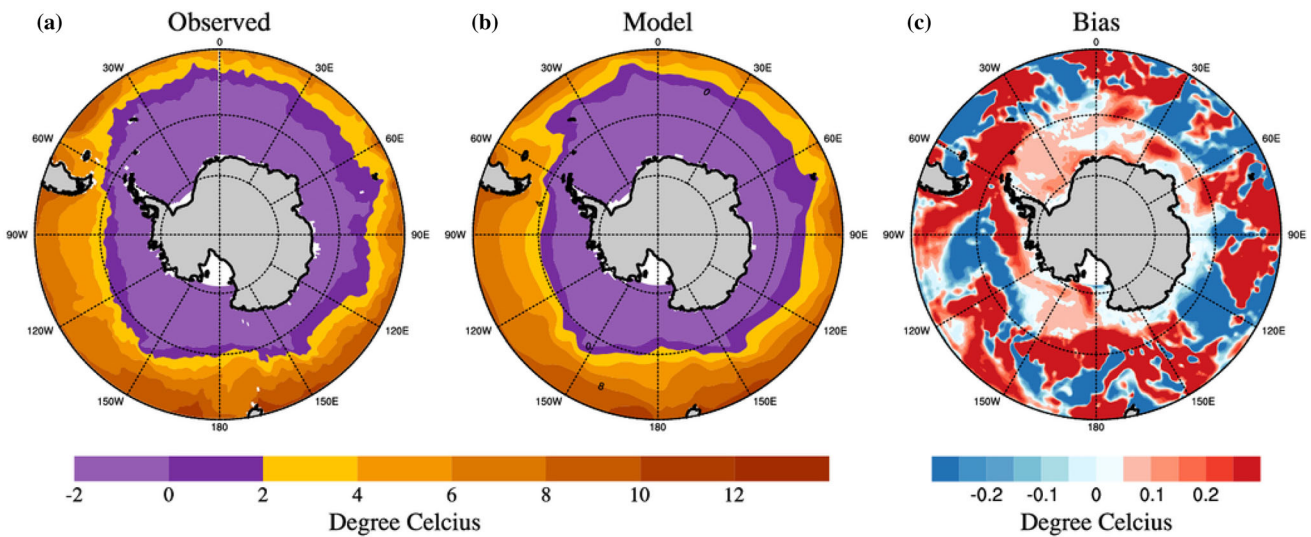


Figure 10. Mean sub-surface temperature at 30 m (JAS) during 1996–2009: (a) observed, (b) model, and (c) bias.

3.4 Predictability of sea-ice extent

Figure 11(a) shows the mean sea-ice extent for the entire simulation period for the months June–October. The sea-ice extent is calculated by integrating the sea-ice regions with more than 15% (0.15, in fraction) of sea-ice concentration, in each grid cell, over the entire southern hemisphere. Observed HadIce sea-ice extent is in good agreement with the simulated sea-ice extent with a correlation value of 0.98. The model sea-ice extent follows the same seasonal pattern as in the observed sea-ice extent. A slight overestimation of the sea-ice extent is consistent with the sea-ice concentration (figure 2). Figure 11(b) shows the

interannual variability of mean JAS sea-ice extent anomaly for the entire simulation period. Out of the 14 JAS seasons from 1996 to 2009, model and observation show opposite signs in the five seasons (1997, 1998, 2000, 2002, 2008), neutral (simulation close to observations) in four seasons (2003, 2005, 2008), and the rest of the six seasons show the similar signs. That means, in approximately 64% of the cases, the model can capture the interannual variability in neutral to extreme cases. The interannual variability in neutral to extreme cases indicates that the model has a good skill and can potentially be used for real-time prediction of sea-ice.

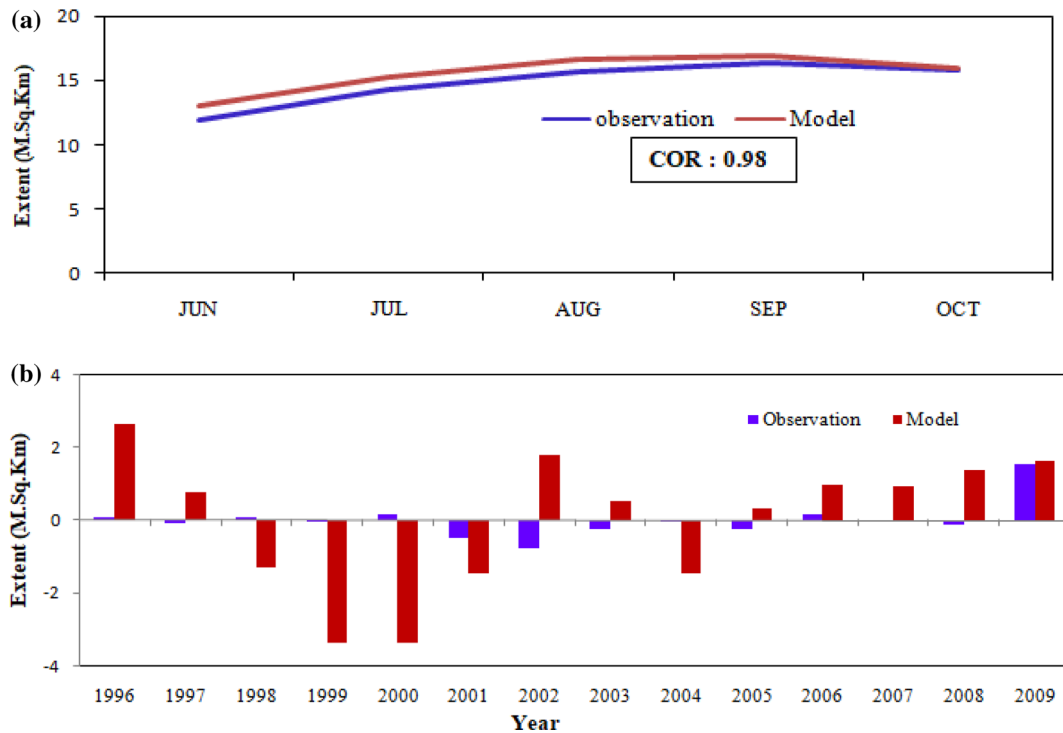


Figure 11. (a) Mean sea-ice extent during 1996–2009. (b) Mean sea-ice (JAS) extent anomaly during 1996–2009.

4. Conclusions and future scope of work

In a coupled modelling system, a better representation of the sea-ice process is essential to include the polar sea-ice interaction with the ocean and atmosphere. In this study, the HadGEM3 global coupled model has been run in seasonal mode (GloSea4) to produce seasonal hindcast for Austral winter. Primarily, the sea-ice variables are evaluated by comparing with available observed satellite and reanalysis datasets. An evaluation of the simulated atmospheric and ocean variables is also conducted to decipher any impacts that the biases in these variables could have on the biases noticed in the sea-ice variables. The seasonal mean/biases of sea-ice concentration, sea-ice thickness, surface currents, sea surface temperature, ice motion vectors, sea-ice extent, 10 m wind, 2 m air temperature, and ocean subsurface temperature are studied. The model could reproduce the sea-ice extent over the Antarctic for the Austral winter seasons with a high correlation value. However, there are moderate biases in the sea-ice concentration. The negative bias in the surface wind was found to impact the surface current ACC. The sea-ice thickness shows a negative bias in most of the sea-ice regions. The simulated SST and the subsurface temperature show a moderate warm bias, impeding the growth rate of sea-ice. The model sea

surface current bias shows a poleward component from the warm bias SST and the subsurface temperature regions. This bias pattern in the surface current could bring warm water from the outer sea-ice regions into the sea-ice region. The sea-ice drift bias away from the sea-ice region is another consistent reason for the negative bias in the sea-ice thickness distribution. Despite moderate biases, the model has high skill in simulating the inter-annual variability of sea-ice extent. Hence, the model is suitable for extended/seasonal prediction of sea-ice during Austral winter. Many of the model biases could be related to the coarser spatial resolution of the atmosphere and ocean components of the model. It is planned to enhance the spatial resolution of the ocean model to 25 km and the atmosphere to 65 km. A multi-layer sea-ice algorithm with enhanced snow process representation will also help more realistic sea-ice simulation even though the realistic ocean, atmosphere, and sea-ice observed data remains a challenge for model validation.

Acknowledgements

ORAP5 ocean reanalysis dataset was taken from <http://marine.copernicus.eu>. ERA-Interim reanalysis was taken from ECMWF. HadISST data was

taken from the Hadley Center, UK. GIOMAS observed sea-ice datasets were taken from Polar Science Centre, University of Washington, USA. NEMO ocean model is part of the NEMO consortium. The CICE model was taken from the Los Alamos National Laboratory sea-ice model repository. The NCMRWF component of the work is done under the MoES Belmont forum project BITMAP.

Author statement

Saheed P P: Conceptualization, methodology, writing original draft, software. Ashis K Mitra, Imranali M Momin and Vimlesh Pant: Writing – review and editing.

References

- Arribas A, Glover M, Maidens A, Peterson K, Gordon M, MacLachlan C, Graham R, Fereday D, Camp J, Scaife A A, Xavier P, McLean P, Colman A and Cusack S 2011 The GloSea4 ensemble prediction system for seasonal forecasting; *Mon. Wea. Rev.* **139** 1891–1910, <https://doi.org/10.1175/2010MWR3615.1>.
- Balmaseda M A, Mogensen K and Weaver A T 2013 Evaluation of the ECMWF ocean reanalysis system ORAS4; *Quart. J. Roy. Meteorol. Soc.* **139** 1132–1161, <https://doi.org/10.1002/qj.2063>.
- Bitz C M and Lipscomb W H 1999 An energy-conserving thermodynamic model of sea ice; *J. Geophys. Res. Ocean.* **104** 15,669–15,677, <https://doi.org/10.1029/1999JC900100>.
- Cavalieri D J and Parkinson C L 2008 Antarctic sea ice variability and trends, 1979–2006; *J. Geophys. Res.* **113** 1–19, <https://doi.org/10.1029/2007JC004564>.
- Dee D P, Uppala S M, Simmons A J, Berrisford P, Poli P, Kobayashi S, Andrae U, Balmaseda M A, Balsamo G, Bauer P, Bechtold P, Beljaars A C M, van de Berg L, Bidlot J, Bormann N, Delsol C, Dragani R, Fuentes M, Geer A J and Vitart F 2011 The ERA-Interim reanalysis: Configuration and performance of the data assimilation system; *Quart. J. Roy. Meteorol. Soc.* **137** 553–597, <https://doi.org/10.1002/qj.828>.
- Feltham D 2015 Arctic sea ice reduction: The evidence, models and impacts; *Phil. Trans. Roy. Soc. A* **373** 1–3, <https://doi.org/10.1098/rsta.2014.0171>.
- Hewitt H T, Copsey D, Culverwell I D, Harris C M, Hill R S R, Keen A B, McLaren A J and Hunke E C 2011 Design and implementation of the infrastructure of HadGEM3: The next-generation Met Office climate modelling system; *Geosci. Model Dev.* **4** 223–253, <https://doi.org/10.5194/gmd-4-223-2011>.
- Hunke E C and Lipscomb W H 2008 CICE: The Los Alamos Sea Ice Model Documentation and Software User's Manual Version 4.0; Los Alamos National Laboratory Tech. Rep. LA-CC-06-012, 76p.
- Madec G and the NEMO team 2008 NEMO ocean engine. Note du Pole de modélisation; Institut Pierre-Simon Laplace (IPSL), France, No 27, ISSN No. 1288-161.
- Parkinson C L and Cavalieri D J 2012 Antarctic sea ice variability and trends, 1979–2010; *Cryosphere* **6** 871–880, <https://doi.org/10.5194/tc-6-871-2012>.
- Parkinson C L 2019 A 40-yr record reveals gradual Antarctic sea ice increases followed by decreases at rates far exceeding the rates seen in the Arctic; *Proc. Natl. Acad. Sci. USA* **116** 14,414–14,423, <https://doi.org/10.1073/pnas.1906556116>.
- Parkinson C L and DiGirolamo N E 2016 New visualizations highlight new information on the contrasting Arctic and Antarctic sea-ice trends since the late 1970s; *Remote Sens. Environ.* **183** 198–204, <https://doi.org/10.1016/j.rse.2016.05.020>.
- Rae J G L, Hewitt H T, Keen A B, Ridley J K, West A E, Harris C M, Hunke E C and Walters D N 2015 Development of the Global Sea Ice 6.0 CICE configuration for the Met Office Global Coupled model; *Geosci. Model Dev.* **8** 2221–2230, <https://doi.org/10.5194/gmd-8-2221-2015>.
- Rayner N A, Parker D E, Horton E B, Folland C K, Alexander L V, Rowell D P, Kent E C and Kaplan A 2003 Global analyses of sea surface temperature, sea ice, and night marine air temperature since the late nineteenth century; *J. Geophys. Res.* **108** 4407, <https://doi.org/10.1029/2002JD002670>.
- Reynolds R W, Smith T M, Liu C, Chelton D B, Casey K S and Schlax M G 2007 Daily high-resolution-blended analyses for sea surface temperature; *J. Clim.* **20** 5473–5496, <https://doi.org/10.1175/2007JCLI1824.1>.
- Saheed P P, Mitra A K, Momin I M, Keen A B, Rajagopal E N, Hewitt H T and Milton S F 2018 Arctic summer sea-ice seasonal simulation with a coupled model: Evaluation of mean features and biases; *J. Earth Syst. Sci.* **128** 1–24, <https://doi.org/10.1007/s12040-018-1043-z>.
- Semtner A J Jr 1976 A model for the thermodynamic growth of sea ice in numerical investigations of climate; *J. Phys. Oceanogr.* **6** 379–389, <https://doi.org/10.1175/1520-0485>.
- Zhang J L and Rothrock D A 2003 Modeling global sea ice with a thickness and enthalpy distribution model in generalized curvilinear coordinates; *Mon. Wea. Rev.* **131** 845–861.